SCIENCE CHINA
Chemistry

•ARTICLES•
SPECIAL TOPIC: Aggregation-induced Emission

August 2018 Vol.61 No.8: 892–897
https://doi.org/10.1007/s11426-018-9287-x

# Multiplexed imaging detection of live cell intracellular changes in early apoptosis with aggregation-induced emission fluorogens

Yabin Zhou[1,2,3†], Haixiang Liu[2†], Na Zhao[2], Zhiming Wang[2], Michael Z. Michael[4], Ni Xie[5], Ben Zhong Tang[2*] & Youhong Tang[3*]

[1]*Faculty of Biological Engineering, Sichuan University of Science and Engineering, Zigong 643000, China;*
[2]*Department of Chemistry, the Hong Kong University of Science and Technology, Hong Kong, China;*
[3]*Centre for NanoScale Science and Technology, College of Science and Engineering, Flinders University, South Australia 5042, Australia;*
[4]*Department of Gastroenterology and Hepatology, Flinders Centre for Innovation in Cancer, Flinders University, South Australia 5042, Australia;*
[5]*AIEgen Biotech Co., Limited, Hong Kong, China*

Received March 21, 2018; accepted May 16, 2018; published online June 19, 2018

Apoptosis is an important process for maintaining tissue homeostasis and eliminating abnormal cells in multicellular organisms. Abnormality in apoptosis often leads to severe diseases such as cancers. Better understanding of its mechanisms and processes is therefore important. Accompanying molecular biology events of apoptosis is a series of cellular morphology changes: nucleus condensation, cell shrinkage and rounding, cell surface blebbing, dynamic blebbing, apoptotic membrane protrusions and nucleus fragmentations and finally, the formation and release of apoptotic bodies. It is difficult to detect cellular changes in the early phase of apoptosis due to the subtle changes at this phase. In the current study, we induced apoptosis in HeLa cells with $H_2O_2$ and used nuclear dye Hoechst 33258, mitochondria, lysosome and cytoplasmic protein specific aggregation-induced emission fluorogens (AIEgens), TPE-Ph-In, 2M-DABS and BSPOTPE to successfully perform live cell multiplexed imaging to investigate early apoptosis cellular events. We showed the gradual dissipation of mitochondria membrane potential until it is non-detectable by TPE-Ph-In. Increased mitophagy detected by TPE-Ph-In and 2M-DABS, condensed nucleus detected by Hoechst 33258, increased permeability and/or reduced integrity of nuclear membrane, and increased intracellular vesicles detected by 2M-DABS are some of the early events of apoptosis.

**apoptosis, multiplexed imaging, HeLa, aggregation-induced emission fluorogens (AIEgens)**

**Citation:** Zhou Y, Liu H, Zhao N, Wang Z, Michael MZ, Xie N, Tang BZ, Tang Y. Multiplexed imaging detection of live cell intracellular changes in early apoptosis with aggregation-induced emission fluorogens. *Sci China Chem*, 2018, 61: 892–897, https://doi.org/10.1007/s11426-018-9287-x

## 1 Introduction

Apoptosis, also called programmed cell death, is an important process for maintaining tissue homeostasis or eliminating abnormal cells in multicellular organisms. An average human adult has more than $10^{13}$ cells [1] and every day around 5 to 70 billion cells die due to apoptosis [2]. Apoptosis is a highly regulated process [3,4]. Its initiation is either intrinsic, through signals such as cytochrome c release from mitochondria due to intracellular stress, or extrinsic, through the activation of certain plasma membrane receptors such as TNF-alpha receptors by external signals [3].

The intrinsic pathway is also known as a mitochondria-initiated pathway [5]. In this pathway, intracellular triggers, such as apoptotic proteins and oxidative stress, can cause the

†These authors contributed equally to this work.
*Corresponding authors (email: tangbenz@ust.hk, youhong.tang@flinders.edu.au)

formation of membrane pores, or they may increase the permeability of the mitochondrial membrane. The result is leakage of apoptotic effectors such as cytochrome c. Once it enters cytoplasm, cytochrome c binds apoptotic protease activating factor 1, procaspase-9 and ATP to form an apoptosome [6]. The apoptosome then sequentially activates caspase-9 and -3, leading to cell death. Accompanying the aforementioned intracellular signalling events is a series of cell morphological changes [7]. Early events of apoptosis include nucleus condensation, cell shrinkage and rounding. These are followed by cell surface blebbing and dynamic blebbing. Subsequently, apoptotic membrane protrusions and nucleus fragmentations may occur, and in the end, there is the formation and release of apoptotic bodies [8–11]. The morphological changes from middle to late phase of apoptosis are quite dramatic and relatively easy to distinguish. However, the morphological changes in early phase of apoptosis are quite subtle and more difficult to identify visually, often requiring the assistance of cellular biochemistry and molecular biology analysis [12].

In this study, our interest was to investigate the subtle cellular changes, especially subcellular organelle changes during the early phase of apoptosis, with the assistance of multiplexed imaging using organelle specific fluorogens, each with unique excitation and emission wavelength. Here we used $H_2O_2$ as a means to induce apoptosis in HeLa cells because it has been shown that $H_2O_2$ induced apoptosis is through an intrinsic pathway [13,14].

A group of unique fluorogens known as aggregation-induced emission fluorogens (AIEgens) has been found to be nonluminescent when molecularly dissolved but highly fluorescent when aggregated. The term AIE describes this novel phenomenon in which restriction of intramolecular motion is the main cause [15–23]. Over the past decade, AIEgens have been successfully employed in a variety of biological and medical research applications [18–20,23], such as dyes specifically labelling membranes [15], mitochondria [16], nuclei [17], etc. Their high specificity in designating organelle, potential to select various excitation/emission wavelengths, strong photo-stability and high biocompatibility make them suitable for multiplexed imaging of live cells [2–6].

## 2 Experimental

### 2.1 Materials

All the chemicals used in this study were purchased from Sigma-Aldrich (USA) unless otherwise specified. DMEM (Cat. No. 11995065), Penicillin-streptomycin (Cat. No. 15140148), Hoechst 33258 (Cat. No. H1398) were obtained from ThermoFisher (USA). BSPOTPE, TPE-Ph-In and 2M-DABS were provided by AIEgen Biotech (Hong Kong, China).

### 2.2 Cell culture

HeLa cells (Cat. No. CCL-2, ATCC) were routinely maintained in DMEM supplemented with 10% FBS and antibiotics (100 units/mL penicillin and 100 g/mL streptomycin) in a 5% $CO_2$ incubator at 37 °C.

### 2.3 $H_2O_2$ treatment

Around 24 h before $H_2O_2$ treatment, $1\times10^5$ of HeLa cells were seeded in a 35 mm petri dish with a cover slip or a plasma-treated 25 mm round cover slip mounted to the bottom of a 35 mm petri dish with an observation window. At the time of treatment, $H_2O_2$ stock was added directly to each dish of the treatment group so that the final concentration of $H_2O_2$ was 5 mM. Cells in each dish were then returned to a 5% $CO_2$ incubator at 37 °C for the designated incubation time.

### 2.4 TPE-Ph-In, 2M-DABS and Hoechst 33258 staining of cells

Sequential staining of the three dyes was performed before the $H_2O_2$ treatment. Media containing 5 μM of TPE-Ph-In staining was first added and incubated for 0.5 h. After removal of the TPE-Ph-In, 5 μM of 2M-DABS containing media was added to the cells and incubated for 0.5 h. After removal of the 2M-DABS, media containing 1 μM of Hoechst 33258 was added to the cells and incubated for 0.5 h. All the incubations were in a 5% $CO_2$ incubator at 37 °C.

### 2.5 TPE-Ph-In, BSPOTPE and 2M-DABS staining of cells

Sequential staining of the three AIEgens was performed after $H_2O_2$ treatment at each time point. HeLa cells were first incubated in HBSS (137 mM NaCl, 5.4 mM KCl, 0.41 mM $MgSO_4$, 0.49 mM $MgCl_2$, 1.26 mM $CaCl_2$, 0.64 mM $KH_2PO_4$, 3 mM $NaHCO_3$, 5.5 mM *D*-glucose, 20 mM HEPES, pH 7.4) containing 200 μM of BSPOTPE for 1 h. BSPOTPE was then replaced by 5 μM of 2M-DABS containing media and cells were further incubated for 0.5 h. 2M-DABS was then removed, followed by the addition of media containing 5 μM of TPE-Ph-In. Cells were further incubated for 0.5 h before imaging on a confocal microscope. All the incubations were carried out in a 5% $CO_2$ incubator at 37 °C.

### 2.6 Multiplexed imaging

The cells were imaged by confocal microscope (Zeiss Laser

Scanning Confocal Microscope; LSM7 DUO, Germany) using ZEN 2009 software (Carl Zeiss). For multiplexed live cell imaging of Hoechst 33258, TPE-Ph-In and 2M-DABS signals, the red channel (TPE-Ph-In) with the excitation wavelength of 489 nm and the emission wavelength of 551–656 nm, the blue channel (Hoechst, Germany) with the excitation wavelength of 405 nm and the emission wavelength of 410–501 nm, and the blue channel (2M-DABS with pseudo-green fluorescence) with the excitation wavelength of 405 nm and the emission wavelength of 519–673 nm were used. For multiplexed live cell imaging of BSPOTPE, TPE-Ph-In and 2M-DABS signals, the red channel (TPE-Ph-In) with the excitation wavelength of 489 nm and the emission wavelength of 551–656 nm, the blue channel (BSPOTPE) with the excitation wavelength of 405 nm and the emission wavelength of 410–501 nm, and the blue channel (2M-DABS with pseudo-green fluorescence) with the excitation wavelength of 405 nm and the emission wavelength of 575–673 nm were used.

## 3 Results and discussion

### 3.1 Mechanisms of selected AIEgens in live cell multiplexed imaging

AIEgens have been used as probes in sensing intracellular organelle changes. In the current study, AIEgens TPE-Ph-In, BSPOTPE and 2M-DABS were used for sensing the changes in mitochondria, cytoplasm and lysosomes simultaneously in HeLa cells during $H_2O_2$ treatment.

TPE-Ph-In, a tetraphenylethylene based cationic AIEgen (Figure 1(a)), could specifically bind negatively charged mitochondria and sense mitochondria membrane potential changes in living cells [16]. Mitochondria membrane potential is a vital indicator for cell health, injury and function. 2M-DABS is a morpholine moiety containing AIEgen that can specifically target lysosome through its affinity with low pH [24] BSPOTPE, a water soluble tetraphenylethylene derivative (Figure 1(b)), has been found to stain cytoplasm through binding hydrophobic cavities of albumin [25] and other cytoplasmic proteins in living cells (Figure S1(a–d), Supporting Information online). In dying, dead or fixed cells, due to the increase of cell membrane permeability, BSPOTPE can also stain cell nuclei (Figure S1(e, f)).

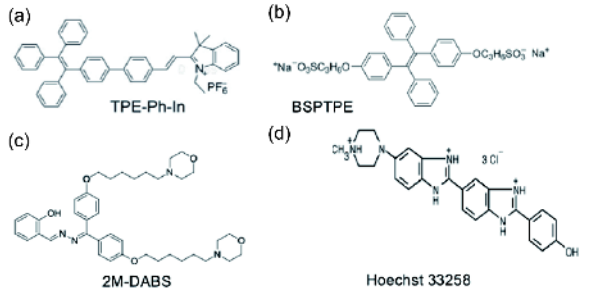


**Figure 1** Structures of AIEgens and Hoechst 33258 used in the multiplexed imaging.

As both BSPOTPE and 2M-DABS can be excited at 405 nm, a lambda scan of emission spectra was performed on a Zeiss confocal microscope for both AIEgens. BSPOTPE had strong emission at 440–565 nm (Figure S2) whereas 2M-DABS had strong emission at 517–632 nm (Figure S3). The excitation wave length of TPE-Ph-In was 489 nm, and a lambda scan showed that a strong emission occurred at 555–661 nm (Figure S4).

### 3.2 $H_2O_2$ treatment and the observation of cellular changes by multiplexed imaging with two AIEgens

$H_2O_2$ is a mediator of apoptosis. There is evidence showing that $H_2O_2$ can trigger apoptosis through down-regulation of anti-apoptotic proteins Bcl-2 and Bcl-XL in mitochondria, up-regulation of apoptotic proteins Bax, Bad and their translocation from cytoplasm to mitochondria [14]. This in turn dissipates mitochondria membrane potential and increases membrane permeability leading to the release of cytochrome c. The release of cytochrome c initiates the formation of apoptosome which then activates caspase-9 and subsequent activation of the effector, caspase-3. There are also observable cellular morphological changes such as nucleus condensation and subsequent fragmentation, membrane blebs and the formation of apoptotic bodies.

We first used 2M-DABS and TPE-Ph-In to stain HeLa cells treated with 5 mM $H_2O_2$ to observe cellular changes during incubation. Figure 2 shows that after 1 h incubation with $H_2O_2$, TPE-Ph-In fluorescence began to decrease, while at 3 h incubation, TPE-Ph-In fluorescence was barely detectable. Since TPE-Ph-In can sense the decrease of mitochondria membrane potential, the decrease in the TPE-Ph-In fluorescence signal (as shown in Figure 2(b, c)) indicates that the incubation with $H_2O_2$ caused a significant decrease of mitochondrial membrane potential. This result is consistent with mitochondria damage by oxidative stress caused by $H_2O_2$ [13], which is an earlier event of apoptosis induced by $H_2O_2$. Our observation of increased mitophagy events (as shown in Figure 2(b, d)) also indicated elevated mitochondria damage caused by $H_2O_2$.

We next used the two aforementioned AIEgens and a commonly used nucleus dye, Hoechst 33258, to further investigate intracellular changes during $H_2O_2$ treatment, as shown in Figure 3. We again observed the decrease in the TPE-Ph-In labelled mitochondrial fluorescence signal with the increase of $H_2O_2$ incubation time. The mitophagy events also increased in $H_2O_2$ treated cells, as shown in Figure 3(e, f). The Hoechst stained nucleus showed condensation after 1 h $H_2O_2$ treatment, as shown in Figure 3(b, c). Apart from this, however, $H_2O_2$ treatment for up to 3 h showed no further

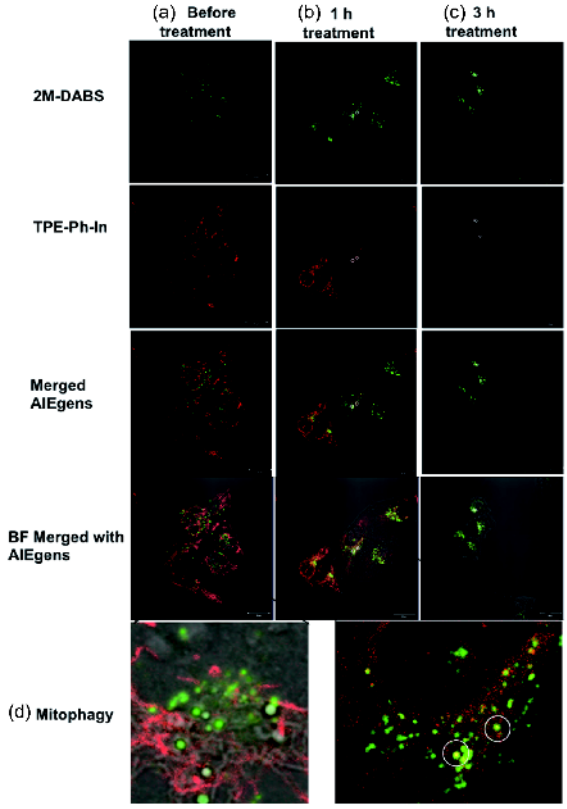


**Figure 2** TPE-Ph-In and 2M-DABS staining of $H_2O_2$ treated HeLa cells. HeLa cells sequentially stained with 2M-DABS and TPE-Ph-In followed by $H_2O_2$ treatment. (a) Images immediately after staining with the two AIEgens; (b) images of cells incubated with $H_2O_2$ for 1 h; (c) images of cells incubated with $H_2O_2$ for 3 h; (d) enlarged regions of interest showing mitophagy at before and 1 h after $H_2O_2$ treatment, with white circles showing region of mitophagy. "BF" stands for "bright field". Scale bar =20 μm (color online).

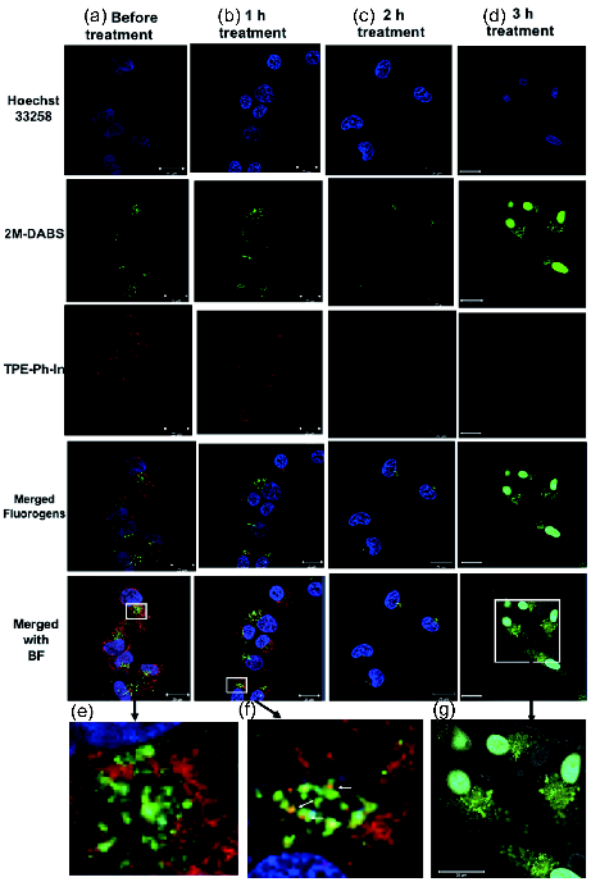


**Figure 3** Multiplexed imaging of $H_2O_2$ treated HeLa cells with two AIEgens and Hoechst 33258. HeLa cells sequentially stained with 2M-DABS, TPE-Ph-In and Hoechst 33258 followed by $H_2O_2$ treatment. (a) Images immediately after staining with the two AIEgens and Hoechst 33258; (b) images of cells incubated with $H_2O_2$ for 1 h; (c) images of cells incubated with $H_2O_2$ for 2 h; (d) images of cells incubated with $H_2O_2$ for 3 h; (e–g) enlarged regions of interest of (a, b, d). White arrows showing mitophagy. "BF" stands for "bright field". Scale bar=20 μm (color online).

nucleus morphology changes such as nucleus fragmentation. Nucleus condensation is one of the intracellular changes during apoptosis which is followed by nucleus fragmentation [8]. There was also a significant increase of Hoechst fluorescence signal within the emission wavelength of 440–503 nm and the excitation wavelength of 405 nm. This caused a signal bleed-through. It could be detected in the 2M-DABS detection wavelength within the emission wavelength of 519–673 nm and the excitation wavelength of 405 nm in which the Hoechst signal could not be detected before $H_2O_2$ treatment. After $H_2O_2$ treatment for 3 h, increased numbers of intracellular vesicles were observable in the bright field, many of which were much larger than the lysosomes detected at other time points. Interestingly, most of these vesicles were 2M-DABS labelled, as shown in Figure 3(d, g).

It is known that during apoptosis, apoptotic bodies form containing either cytosolic content or fragmented nucleus. These 2M-DABS labelled vesicles could potentially be apoptotic bodies. It has been shown that during apoptosis, lysosomal membrane permeability increases, causing its content to leak into the cytoplasm [24]. This lysosomal leakage can lead to a decrease in cytoplasmic pH, which may explain why these vesicles could be labelled by 2M-DABS which has affinity to the low pH. No Hoechst signal was detected in these vesicles, indicating the absence of nucleus content. This finding is consistent with the absence of any nucleus fragmentation detected by Hoechst at this time point.

### 3.3 Multiplexed imaging of intracellular changes during $H_2O_2$ treatment with three AIEgens

We further used BSPOTPE, 2M-DABS and TPE-Ph-In to detect HeLe cell intracellular changes during $H_2O_2$ treatment. In our previous study, we found that water soluble BSPOTPE would only stain cytoplasmic proteins and could not enter the nucleus in healthy cells (Figure S1(a–d)).

However, it could stain the nucleus in dying or dead cells (Figure S1(e)). We speculated that this was due to the increase in the permeability of the nuclear membrane.

In the current study, we first treated cells with 5 mM $H_2O_2$ for the designated time, then performed cell staining with the AIEgens. In healthy cells before treatment there was no BSPOTPE fluorescence in the nucleus, as shown in Figure 4(a). A proportion of BSPOTPE fluorescence signals were found co-localized with those of 2M-DABS and TPE-Ph-In, as shown in Figure 4(a). This result is consistent with our previous finding and our speculation that BSPOTPE binds to hydrophobic cavities of cellular proteins regardless of their location (excluding the nucleus), so that it should be detected in cytoplasm and various cellular organelle. For instance, we have detected its presence in plasma membrane, lipid droplets.

When cells were treated with $H_2O_2$ for as little as 2 h, BSPOTPE signal could be detected in the nucleus of some cells, as shown in Figure 4(b–e). This suggests that $H_2O_2$ treatment could significantly increase the permeability of the nuclear envelope and trigger cell death after as short as 2 h. Interestingly, the signal is very strong in certain areas with dot-like shapes, some cells having only one such shape while others had two or more. Since there is no evidence showing that BSPOTPE can bind DNA, this could be some protein-rich sub-nuclear structure.

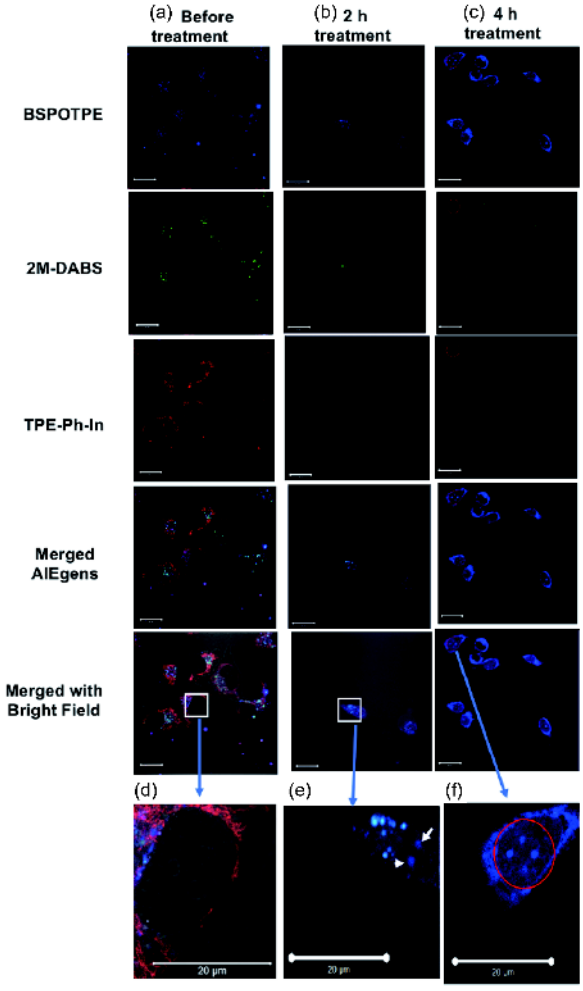


**Figure 4** Multiplexed imaging of $H_2O_2$ treated HeLa cells with three AIEgens. HeLa cells sequentially stained with 2M-DABS, TPE-Ph-In and BSPOTPE followed by $H_2O_2$ treatment. (a) Images immediately after staining with the three AIEgens; (b) images of cells incubated with $H_2O_2$ for 2 h; (c) images of cells incubated with $H_2O_2$ for 4 h; (d–f) enlarged regions of interest of (a–c) showing nucleus staining by BSPOTPE. Scale bar=20 μm (color online).

## 4 Conclusions

In this article, we utilised multiplexed imaging on HeLa cells stained with a combination of TPE-Ph-In, 2M-DABS and Hoechst 33258 or TPE-Ph-In, 2M-DABS and BSPOTPE to investigate intracellular changes during early and mid-apoptosis. When using TPE-Ph-In, 2M-DABS and Hoechst 33258 to perform continuous and simultaneous detection of mitochondria, lysosome and nucleus changes during early to mid- apoptosis were induced by $H_2O_2$ treatment in the same batch of cells. Our data suggests that 5 mM $H_2O_2$ treatment for 1 h was sufficient to decrease mitochondrial membrane potential, increase mitophagy events and cause nucleus condensation. $H_2O_2$ treatment for 2 h could result in a potential decrease of mitochondria membrane to a level undetectable by TPE-Ph-In, while nucleus morphology did not show observable changes. Further $H_2O_2$ treatment for 3 h induced a large number of 2M-DABS stained vesicles that could potentially be apoptotic bodies. The use of TPE-Ph-In, 2M-DABS and BSPOTPE to perform simultaneous endpoint detection at each time point of $H_2O_2$ treatment showed that the changes in mitochondria and lysosome were similar to that detected by the aforementioned continuous detection. BSPOTPE detection of nucleus changes revealed that nuclear membrane permeability significantly increased at 2 h treatment by $H_2O_2$.

**Acknowledgements** This work was supported by the Hong Kong Branch of Chinese National Engineering Research Centres for Tissue Restoration and Reconstruction. We acknowledged the use of South Australian nodes of the Australian Microscopy & Microanalysis Research Facility and the Australian National Fabrication Facility at Flinders University.

**Conflict of interest** The authors declare that they have no conflict of interest.

**Supporting information** The supporting information is available online at http://chem.scichina.com and http://link.springer.com/journal/11426. The supporting materials are published as submitted, without typesetting or editing. The responsibility for scientific accuracy and content remains entirely with the authors.

1 Alberts B, Johnson A, Lewis J, Morgan D, Raff M, Roberts K, Walter P. *Molecular Biology of the Cell*. 6th ed. New York: Garland Science, 2015. 2
2 Karam JA. *Apoptosis in Carcinogenesis and Chemotherapy*. Berlin: Springer, 2009
3 Slattery ML, Mullany LE, Sakoda LC, Wolff RK, Samowitz WS, Herrick JS. *Apoptosis*, 2018, 23: 237–250
4 Fuchs Y, Steller H. *Cell*, 2011, 147: 742–758

5 McArthur K, Whitehead LW, Heddleston JM, Li L, Padman BS, Oorschot V, Geoghegan ND, Chappaz S, Davidson S, San Chin H, Lane RM, Dramicanin M, Saunders TL, Sugiana C, Lessene R, Osellame LD, Chew TL, Dewson G, Lazarou M, Ramm G, Lessene G, Ryan MT, Rogers KL, van Delft MF, Kile BT. *Science*, 2018, 359: eaao6047
6 Shi Y. *Methods Enzymol*, 2008, 442: 141–156
7 Tinari A, Giammarioli AM, Manganelli V, Ciarlo L, Malorni W. *Methods Enzymol*, 2008, 442: 1–26
8 Tixeira R, Caruso S, Paone S, Baxter AA, Atkin-Smith GK, Hulett MD, Poon IKH. *Apoptosis*, 2017, 22: 475–477
9 Atkin-Smith GK, Paone S, Zanker DJ, Duan M, Phan TK, Chen W, Hulett MD, Poon IKH. *Sci Rep*, 2017, 7: 39846
10 Coleman ML, Sahai EA, Yeo M, Bosch M, Dewar A, Olson MF. *Nat Cell Biol*, 2001, 3: 339–345
11 Wickman G, Julian L, Olson MF. *Cell Death Differ*, 2012, 19: 735–742
12 Banfalvi G. *Apoptosis*, 2017, 22: 306–323
13 Chernyak BV, Izyumov DS, Lyamzaev KG, Pashkovskaya AA, Pletjushkina OY, Antonenko YN, Sakharov DV, Wirtz KWA, Skulachev VP. *Biochim Biophys Acta*, 2006, 1757: 525–534
14 Singh M, Sharma H, Singh N. *Mitochondrion*, 2007, 7: 367–373
15 Li Y, Wu Y, Chang J, Chen M, Liu R, Li F. *Chem Commun*, 2013, 49: 11335
16 Zhao N, Chen S, Hong Y, Tang BZ. *Chem Commun*, 2015, 51: 13599–13602
17 Yu CYY, Zhang W, Kwok RTK, Leung CWT, Lam JWY, Tang BZ. *J Mater Chem B*, 2016, 4: 2614–2619
18 Cheng Y, Dai J, Sun C, Liu R, Zhai T, Lou X, Xia F. *Angew Chem Int Ed*, 2018, 57: 3123–3127
19 Cheng Y, Sun C, Ou X, Liu B, Lou X, Xia F. *Chem Sci*, 2017, 8: 4571–4578
20 Cheng Y, Huang F, Min X, Gao P, Zhang T, Li X, Liu B, Hong Y, Lou X, Xia F. *Anal Chem*, 2016, 88: 8913–8919
21 Xu X, Huang J, Li J, Yan J, Qin J, Li Z. *Chem Commun*, 2011, 47: 12385–12387
22 Li Q, Li Z. *Sci China Chem*, 2015, 58: 1800–1809
23 Liang J, Feng G, Kwok RTK, Ding D, Tang B, Liu B. *Sci China Chem*, 2016, 59: 53–61
24 Nilsson C, Kågedal K, Johansson U, Öllinger K. *Methods Cell Sci*, 2003, 25: 185–194
25 Tong H, Hong Y, Dong Y, Häussler M, Li Z, Lam JWY, Dong Y, Sung HHY, Williams ID, Tang BZ. *J Phys Chem B*, 2007, 111: 11817–11823